Available online at www.sciencedirect.com
ScienceDirect
Trans. Nonferrous Met. Soc. China 23(2013) 2568−2576
Transactions of Nonferrous Metals Society of China
www.tnmsc.cn

Effects of Gd on microstructure and mechanical property of ZK60 magnesium alloy

Zheng-hua HUANG, Wen-jun QI, Jing XU

Guangzhou Research Institute of Non-ferrous Metals, Guangzhou 510650, China

Received 12 July 2012; accepted 15 November 2012

Abstract: Microstructures and phase compositions of as-cast and extruded ZK60−*x*Gd (*x*=0−4) alloys were investigated. Meanwhile, the tensile mechanical property was tested. With increasing the Gd content, as-cast microstructure is refined gradually. Mg−Zn−Gd new phase increases gradually, while $MgZn_2$ phase decreases gradually to disappear. The second phase tends to distribute along grain boundary by continuous network. As-cast tensile mechanical property is reduced slightly at ambient temperature when the Gd content does not exceed 2.98%. After extrusion by extrusion ratio of 40 and extrusion temperature of 593 K, microstructure is refined further with decreasing the average grain size to 2 μm for ZK60−2.98Gd alloy. Broken second phase distributes along the extrusion direction by zonal shape. Extruded tensile mechanical property is enhanced significantly. Tensile strength values at 298 and 473 K increase gradually from 355 and 120 MPa for ZK60 alloy to 380 and 164 MPa for ZK60−2.98Gd alloy, respectively. Extruded tensile fractures exhibit a typical character of ductile fracture.

Key words: ZK60 magnesium alloy; Gd modification; extrusion; microstructure; mechanical property; fracture morphology

1 Introduction

Magnesium alloys with high specific strength are used widely in automotive, communicated, electronic and aerial industries [1]. Wrought magnesium alloys exhibit higher strength, better ductility and comprehensive property; however, their plasticity is still relatively poor owing to the limit of crystal structure (hexagonal close packed, HCP) [2]. Therefore, it is necessary to develop new wrought magnesium alloys with high performance by investigating the deformation mechanism.

Rare earth (RE) with unique atomic electron and chemical property can purify alloy melt, ameliorate the microstructure and enhance the mechanical property effectively. Researchers had extensively studied the effects of Y [3−5], Ce [6], Nd [7], Yb [8] and Ho [9] on the microstructure and tensile mechanical property of ZK60 alloy, being one of the most widely used wrought magnesium alloys currently. Gd was commonly used to develop Mg−Gd−Y series heat-resistant magnesium alloys [10−13]; however, its effects on the microstructure and tensile mechanical property of ZK60 alloy had been rarely studied yet. As well as grain size, the morphology, distribution and volume fraction of second phase can also affect the tensile mechanical property of magnesium alloys significantly [7]. Therefore, the present work is focused on studying the microstructures and tensile mechanical properties of as-cast and extruded ZK60−*x*Gd (*x*=0−4) alloys in detail, and then discussing the role of grain size and second phase on the strengthening and deformation mechanism.

2 Experimental

Chemical compositions of as-cast ZK60−*x*Gd alloys measured by inductively coupled plasma analyzer (ICP, JY Ultima2) are listed in Table 1. Alloy ingots were prepared by melting pure Mg, pure Zn and Mg−30%Zr, Mg−20%Gd master alloys in electric resistance furnace under the mixed atmosphere of CO_2 and SF_6. When the melt temperature of pure Mg reached 1003 K, pure Zn and two master alloys were added into the melt in turn. Then, the melt was stirred twice within 1 h to ensure the compositional homogeneity. After adding refine agent (JDMJ), the melt was held at 1033 K for 30 min. When the temperature cooled to 988 K, the melt was poured into the wedge permanent mold with preheated temperature of 523 K, and then as-cast samples were

Foundation item: Projects (2010A090200078, 2011A080403008) supported by the Major Science and Technology Project of Guangdong Province, China
Corresponding author: Zheng-hua HUANG; Tel/Fax: +86-20-37238039; E-mail: zhhuang@live.cn
DOI: 10.1016/S1003-6326(13)62769-7

Table 1 Chemical composition of ZK60−*x*Gd alloys (mass fraction, %)

Alloy	Zn	Zr	Gd	Mg
ZK60	5.83	0.66	−	Bal.
ZK60−0.28Gd	5.90	0.61	0.28	Bal.
ZK60−1.00Gd	6.07	0.54	1.00	Bal.
ZK60−1.94Gd	6.22	0.57	1.94	Bal.
ZK60−2.98Gd	6.27	0.57	2.98	Bal.
ZK60−3.81Gd	6.00	0.65	3.81	Bal.

obtained. Cast rods obtained under the same technology were homogenized at 673 K for 8 h in the heat-treating furnace, and then machined to a diameter of 100 mm. Extrusion rods were obtained by extruder with extrusion ratio λ, extrusion temperature T and extrusion speed v of 40, 593 K and 1−2 m/min, respectively.

The as-cast and extruded specimens were etched with 4% HNO_3 (volume fraction) in ethanol and a solution of 1.5 g picric acid, 25 mL ethyl alcohol, 5 mL acetic acid plus 10 mL distilled water, respectively. Microstructural observation was carried out on an optical microscope (OM, Leica DM IRM), scanning electron microscope (SEM, JEOL JXA−8100) with energy dispersive spectroscopy (EDS, OXFORD 7412) and transmission electron microscope (TEM, Tecnai G^2 20). Phase analysis was carried out on an X-ray diffractometer (XRD, D/MAX-RC) with Cu K_α radiation. Phase change during the heating process was characterized by isochronally heating in a differential scanning calorimeter (DSC, Netzsch STA409) under flow of highly-purified Ar atmosphere at a rate of 20 K/min. Tensile test at the temperature ranging from 298 K to 473 K was performed on a test machine (GP-TS2000) at a rate of 2 mm/min. Tensile fractographs were observed using SEM.

3 Results

3.1 Microstructure and mechanical property of as-cast alloy

Figures 1 and 2 show the optical graphs and SEM

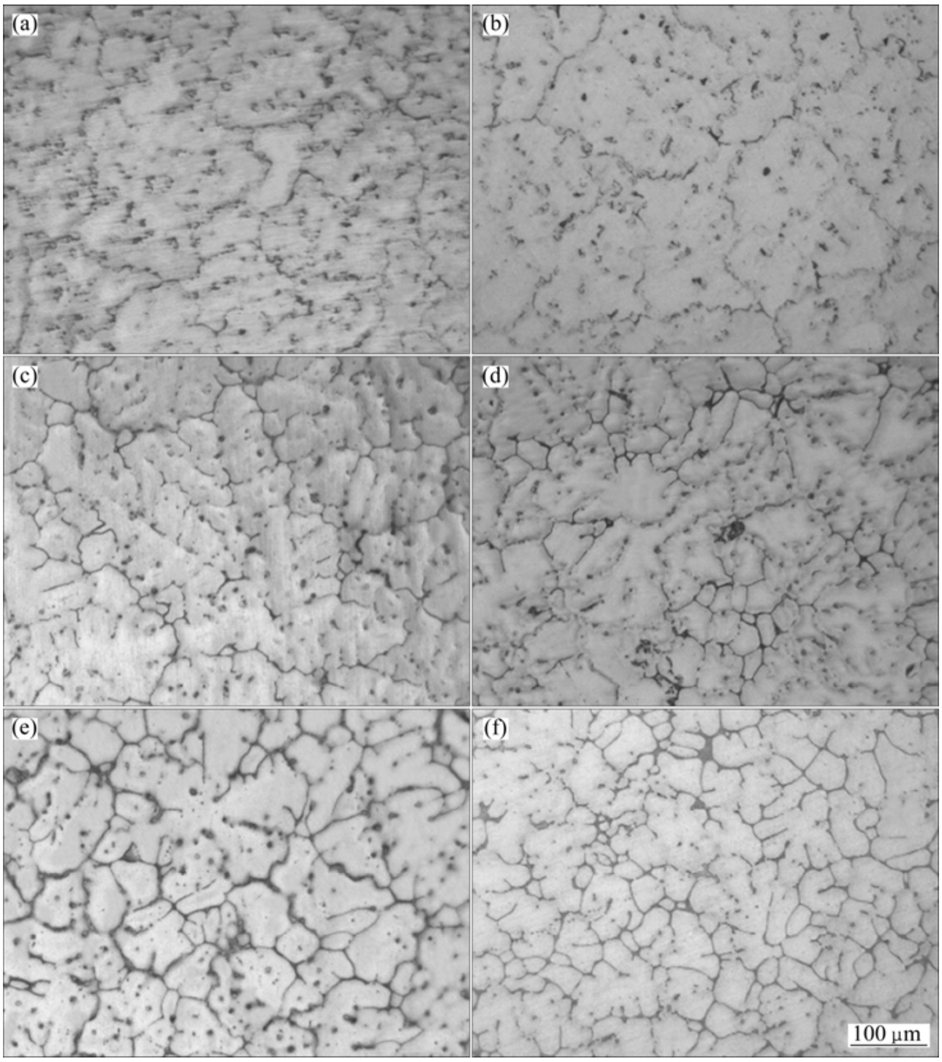

Fig. 1 Optical graphs of as-cast ZK60−*x*Gd alloys: (a) ZK60; (b) ZK60−0.28Gd; (c) ZK60−1.00Gd; (d) ZK60−1.94Gd; (e) ZK60−2.98Gd; (f) ZK60−3.81Gd

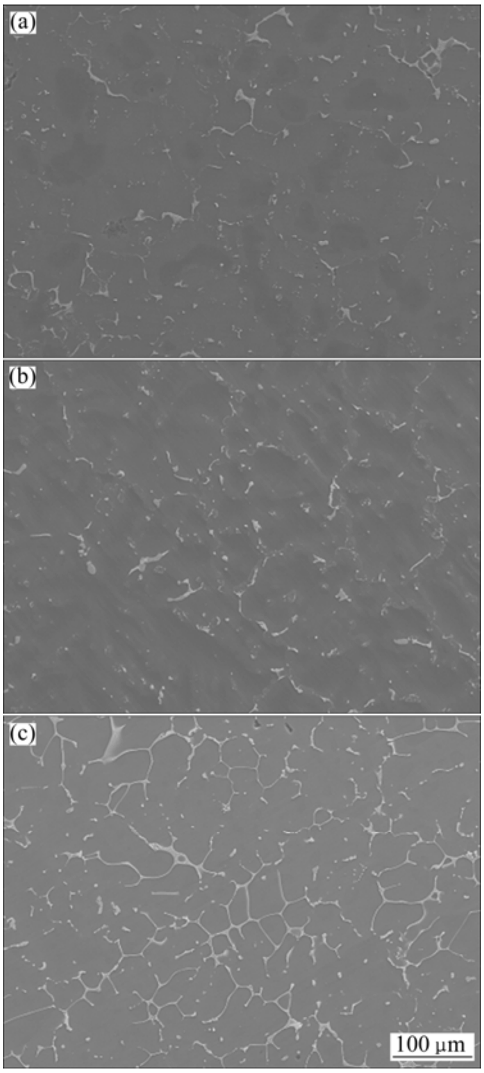

Fig. 2 SEM images of as-cast ZK60−*x*Gd alloys: (a) ZK60; (b) ZK60−0.28Gd; (c) ZK60−2.98Gd

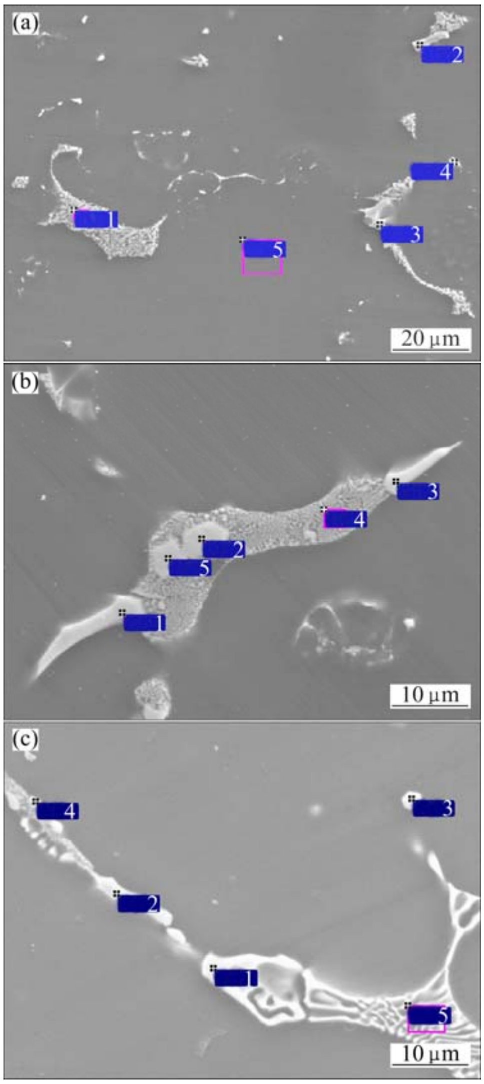

Fig. 3 EDS spectra of as-cast ZK60−*x*Gd alloys: (a) ZK60; (b) ZK60−0.28Gd; (c) ZK60−2.98Gd

images of as-cast alloys, respectively. As-cast ZK60 alloy exhibits coarse microstructure and few dispersed second phases. With increasing the Gd content, as-cast microstructure is refined gradually. Meanwhile, the second phase increases gradually and tends to distribute along grain boundary by continuous network.

Figure 3 shows the EDS spectra of as-cast alloys and the results are listed in Table 2. For as-cast ZK60 alloy, there exist two different Mg−Zn phases containing relatively low and high Zr contents, respectively, while new Mg−Zn−Gd plus Mg−Zn and only Mg−Zn−Gd phases can be observed for as-cast ZK60−0.28Gd and ZK60−2.98Gd alloys, respectively. However, mole fraction in Mg−Zn phase is slightly different from $MgZn_2$ phase determined by following XRD patterns owing to the affection by adjacent α-Mg matrix, and that in Mg−Zn−Gd phase changes slightly with most of the Gd content of about 5% in mole fraction. Majority of element Zn distributes along grain boundary to form

Table 2 EDS results of as-cast ZK60−*x*Gd alloys

Alloy	Position in Fig. 3	*x*(Mg)/%	*x*(Zn)/%	*x*(Zr)/%	*x*(Gd)/%
ZK60	Spectrum 1	61.87	38.06	0.07	
	Spectrum 2	21.11	60.29	18.60	
	Spectrum 3	30.15	54.58	15.27	
	Spectrum 4	72.78	26.97	0.25	
	Spectrum 5	98.26	1.60	0.14	
ZK60−0.28Gd	Spectrum 1	64.66	32.17		3.17
	Spectrum 2	37.63	56.85		5.52
	Spectrum 3	49.74	45.88		4.37
	Spectrum 4	68.61	31.39		
	Spectrum 5	37.30	57.15		5.56
ZK60−2.98Gd	Spectrum 1	42.23	40.13		17.64
	Spectrum 2	50.45	43.57		5.98
	Spectrum 3	66.47	29.50		4.03
	Spectrum 4	72.40	25.85		1.74
	Spectrum 5	77.13	16.24		6.63

$MgZn_2$ phase for as-cast ZK60 alloy. Similar to element Zn, element Gd also mainly does along grain boundary to form Mg−Zn−Gd phase for as-cast ZK60−2.98Gd alloy (see Fig. 4).

In order to determine new phase owing to the addition of Gd, the comparison between the XRD spectra of as-cast ZK60 and ZK60−2.98Gd alloys was made (see Fig. 5(a)). XRD pattern of as-cast ZK60 alloy consists of the peaks of α-Mg and $MgZn_2$ phases, while the peak of $MgZn_2$ phase disappears completely and that of an unknown phase, not Mg−Gd binary phase, can be observed in the XRD pattern of as-cast ZK60−2.98Gd alloy. Combined with the EDS results, the phase is considered Mg−Zn−Gd phase. This indicates that added Gd atoms combine with Mg and Zn atoms to form Mg−Zn−Gd new phase on the priority.

Figure 5(b) shows the isochronal heating DSC curves of as-cast alloys and peak temperatures T_{Pi} of endothermic peaks are listed in Table 3. For as-cast ZK60 alloy, there exist two distinct endothermic peaks with T_{P1} and T_{P2} of 618 and 902 K, respectively, which are close to the melting point T_m (620 and 923 K) of $MgZn_2$ phase and α-Mg matrix, respectively. Thus the two endothermic peaks should be corresponding to the melting of the two phases, respectively. For as-cast ZK60−0.28Gd alloy, the two endothermic peaks still

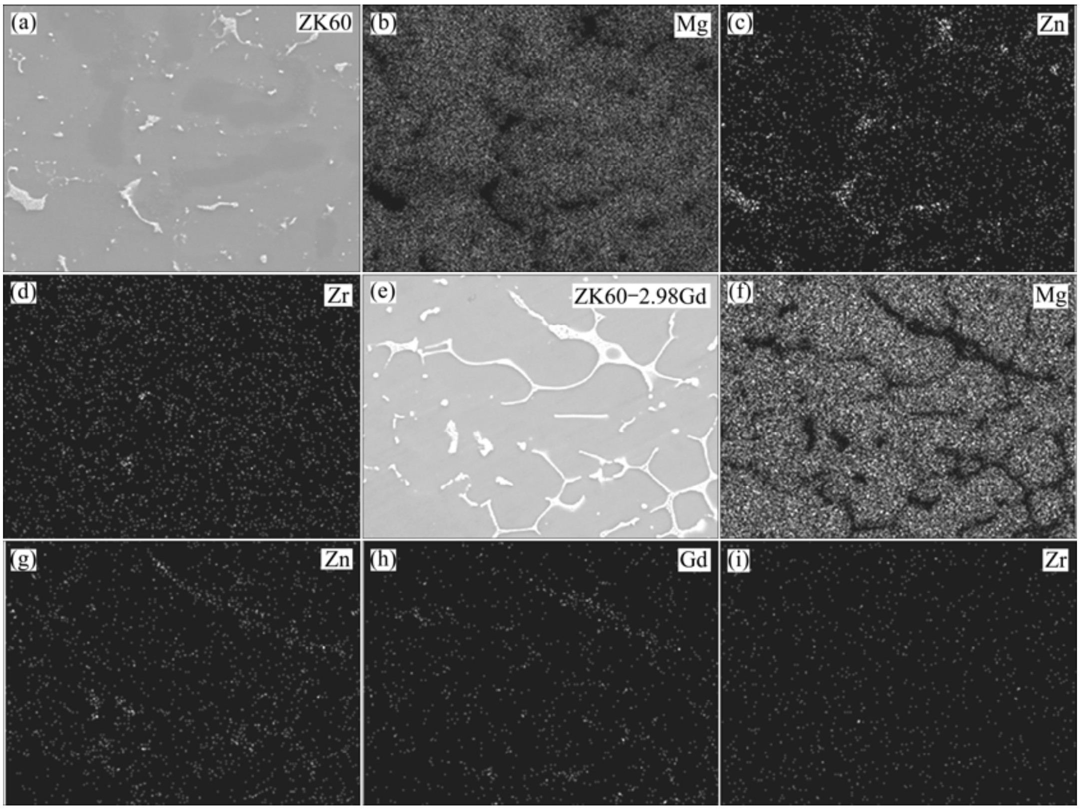

Fig. 4 Distribution of elements in as-cast microstructures of ZK60−*x*Gd alloys: (a, b, c, d) ZK60; (e, f, g, h, i) ZK60−2.98Gd

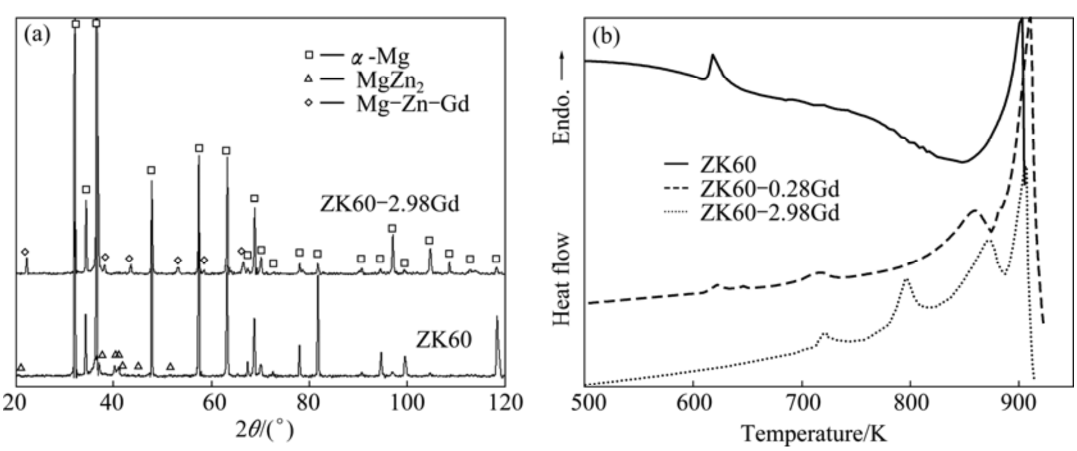

Fig. 5 XRD patterns (a) and isochronal heating DSC curves (b) of as-cast ZK60−*x*Gd alloys

Table 3 Peak temperature T_{Pi} on isochronal heating DSC curves of as-cast ZK60−*x*Gd alloys

Alloy	T_{P1}/K	T_{P2}/K	T_{P3}/K	T_{P4}/K
ZK60	618	902	−	−
ZK60−0.28Gd	622	717	859	910
ZK60−2.98Gd	718	796	871	905

exist with the significantly weak first one, and meanwhile two new ones occur at T_P=717 and 859 K, respectively. For as-cast ZK60−2.98Gd alloy, the endothermic peak at T_P≈620 K disappears completely and another new one occurs at T_P=796 K on the basis of retaining others. These endothermic peaks existing at the peak temperature ranging from 717 K to 871 K for the two Gd-containing alloys should be corresponding to the melting of Mg−Zn−Gd phase. This indicates that Mg−Zn−Gd phase exhibits higher thermal stability than $MgZn_2$ phase.

For as-cast alloys at ambient temperature, tensile strength σ_b first decreases gradually from 225 MPa for ZK60 alloy to 194 MPa for ZK60−1.00Gd alloy, then slightly increases to 205 MPa for ZK60−2.98Gd alloy, and finally significantly decreases to 172 MPa for ZK60−3.81Gd alloy. Elongation δ is not lower than 7.5% when the Gd content does not exceed 2.98% and significantly decreases to 3.5% for ZK60−3.81Gd alloy (see Fig. 6(a)). In summary, as-cast tensile mechanical property is reduced slightly at ambient temperature when the Gd content does not exceed 2.98%. All as-cast tensile fractures exhibit a complex mode of ductile and brittle fractures (see Figs. 7(a), (c) and (e)). Dimples occupy the majority, while cleavage steps are few for as-cast ZK60 alloy. It is contrary for as-cast ZK60−0.28Gd alloy, which is consistent with the slight decrease in elongation. No cleavage step exists for as-cast ZK60−2.98Gd alloy. Meanwhile, the increasing dimples are still less than those for as-cast ZK60 alloy, which is consistent with the slightly lower tensile mechanical property.

3.2 Microstructure and mechanical property of extruded alloy

ZK60, ZK60−0.28Gd and ZK60−2.98Gd alloys were chosen to study the extruded microstructure and tensile mechanical property in the present work. Optical, SEM and TEM images in the extrusion direction are shown in Figs. 8 and 9, respectively. Compared with as-cast state, extruded microstructure is refined significantly owing to the dynamic recrystallization during the hot deformation process. For extruded ZK60 alloy, dynamic recrystallization grains (DRGs) change at a size ranging from 2 μm to 10 μm with average grain size $\bar{d}$ of 5 μm. Meanwhile, majority of $MgZn_2$ phase dissolved through homogenization does not re-precipitate during the hot deformation process. With increasing the Gd content, DRGs become unique and $\bar{d}$ gradually decreases to 2 μm for extruded ZK60−2.98Gd alloy. Meanwhile, broken second phase tends to distribute along the extrusion direction by zonal shape, especially for extruded ZK60−2.98Gd alloy. Diffraction spots to the particles in the two alloys are corresponding to Mg−Zn phase containing relatively high Zr content and Mg−Zn−Gd phase, respectively.

Compared with as-cast state, extruded tensile mechanical property is enhanced significantly at ambient temperature (see Fig. 6(b)). σ_b and δ reach 355 MPa and 19.5% for extruded ZK60 alloy, respectively. As the Gd content increases, σ_b increases gradually to 380 MPa for extruded ZK60−2.98Gd alloy, while δ gradually decreases to 7%, which is even slightly lower than as-cast value. With increasing the test temperature, σ_b decreases gradually, while δ increases gradually. For extruded ZK60 alloy, σ_b decreases to 157 and 120 MPa at 448 and 473 K, respectively, indicating that its application temperature can be considered 448 K. Extruded ZK60−0.28Gd alloy exhibits slightly larger values of σ_b at each test temperature, while extruded ZK60−2.98Gd alloy has significantly larger values where

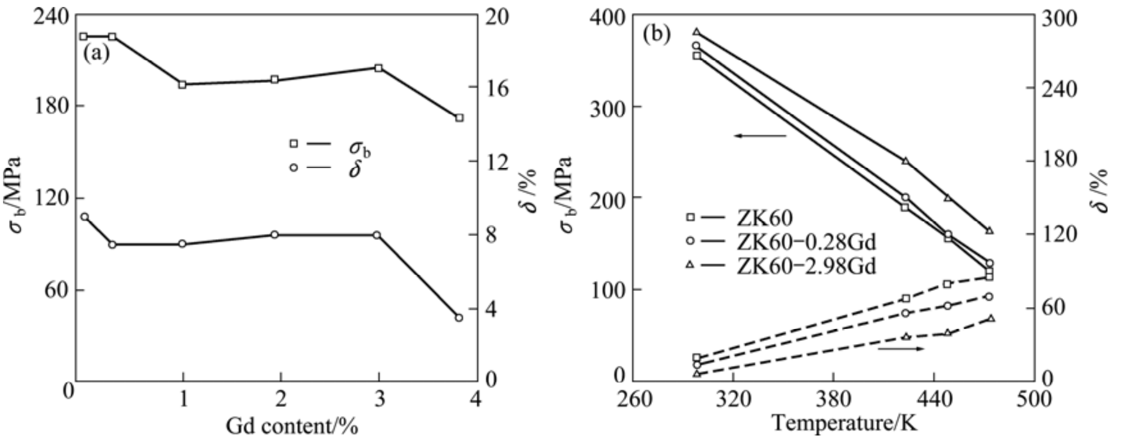

Fig. 6 Tensile mechanical properties of as-cast and extruded ZK60−*x*Gd alloys: (a) *T*=298 K, as-cast alloy; (b) Extruded alloy

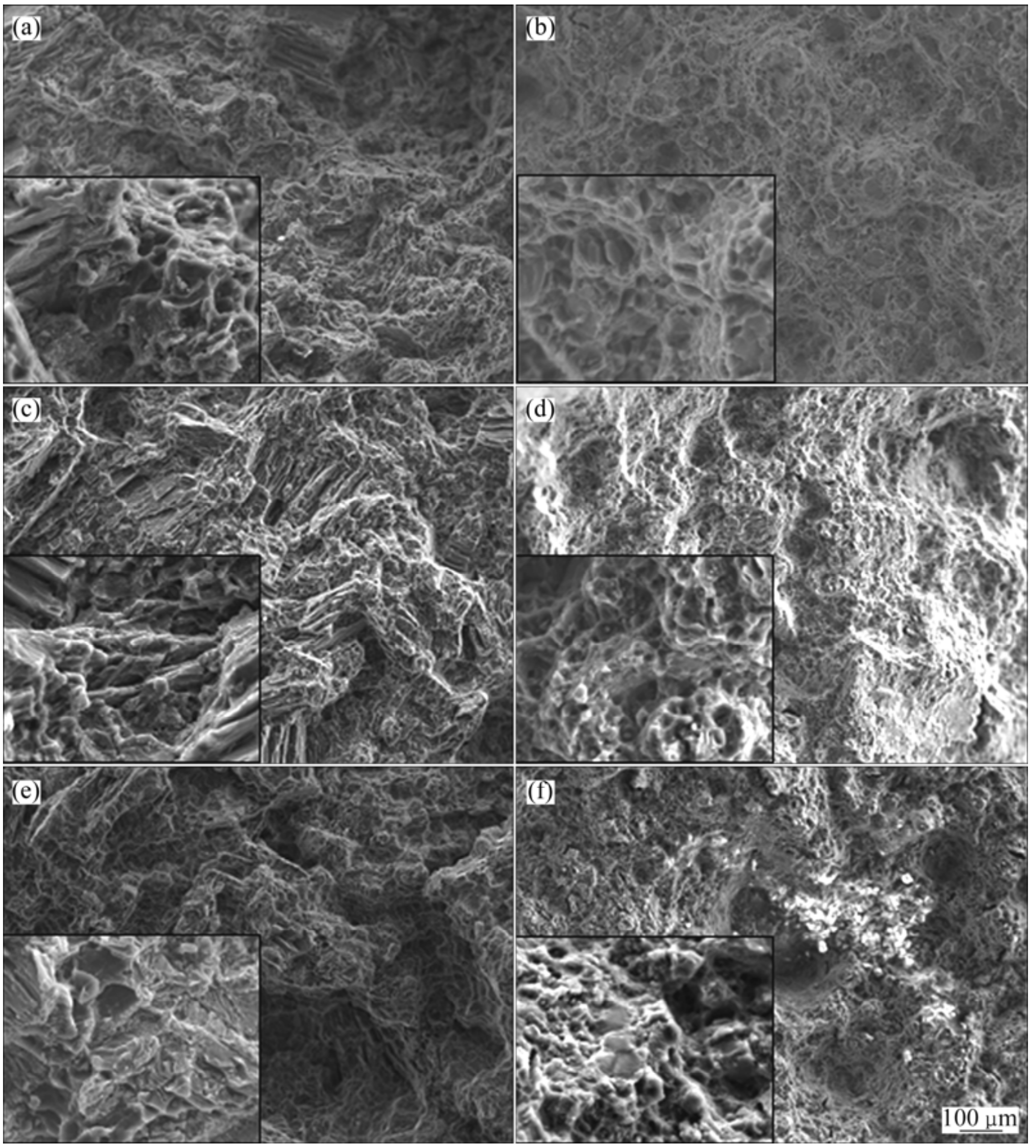

Fig. 7 SEM morphologies of tensile fractures at ambient temperature of as-cast and extruded ZK60−*x*Gd alloys (Illustrations indicate the local enlarged regions): (a) As-cast ZK60; (b) Extruded ZK60; (c) As-cast ZK60−0.28Gd; (d) Extruded ZK60−0.28Gd; (e) As-cast ZK60−2.98Gd; (f) Extruded ZK60−2.98Gd

σ_b reaches 164 MPa at 473 K, indicating that its application temperature is enhanced to 473 K. Meanwhile, the increase in the Gd content still reduces the value of δ at each test temperature. In summary, the addition of Gd can enhance the tensile mechanical properties of extruded ZK60 alloy at ambient and elevated temperatures. All extruded tensile fractures at ambient temperature exhibit a typical character of ductile fracture (see Figs. 7(b), (d) and (f)). For extruded ZK60 alloy, uniform and deep dimples occupy the majority and meanwhile few fine second phase particles can be observed at the bottom of dimples. Dimples become less and shallow; meanwhile second phase particles increase gradually with increasing the Gd content, which is consistent with the gradual decrease in the elongation. Combined with as-cast results, the second phase particles at the bottom of dimples should be $MgZn_2$ and Mg−Zn−Gd phases.

4 Discussion

4.1 Phase composition

Degree of difficulty in forming compounds between different elements can be judged by electronegativity difference $\Delta\chi$. The greater the value of $\Delta\chi$ is, the larger the binding force is and then the easier the formation of compounds is [14]. Electronegativities χ are 1.31, 1.65 and 1.20 for Mg, Zn and Gd, respectively [15], thus Zn−Gd exhibits the larger value of $\Delta\chi$ (0.45) than Mg−Zn and Mg−Gd (0.34 and 0.11, respectively). Thus

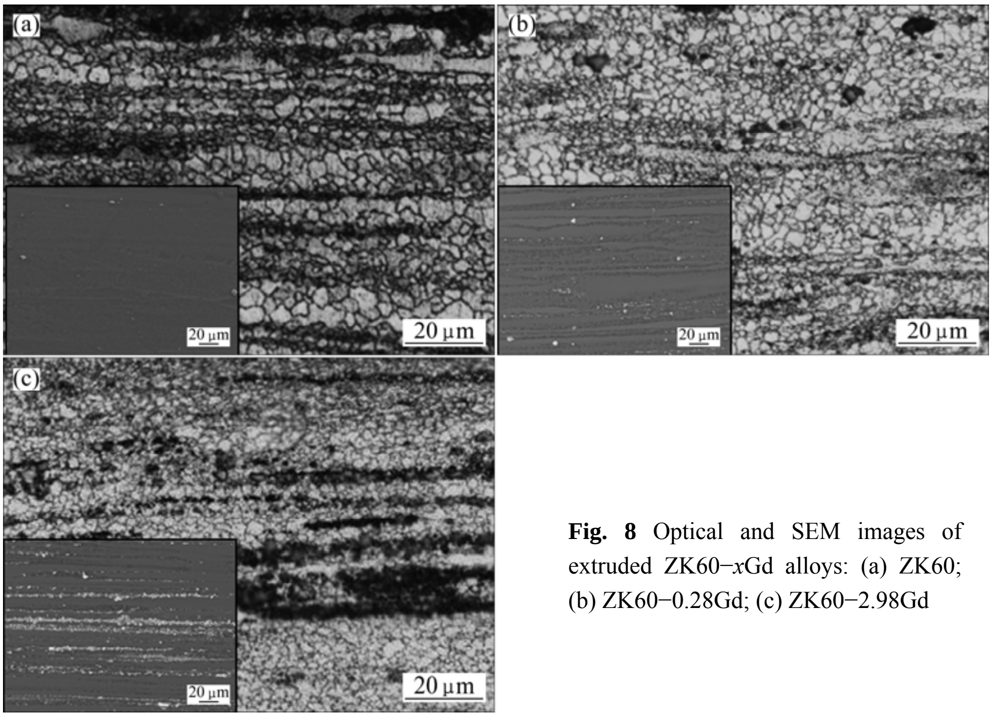

Fig. 8 Optical and SEM images of extruded ZK60−*x*Gd alloys: (a) ZK60; (b) ZK60−0.28Gd; (c) ZK60−2.98Gd

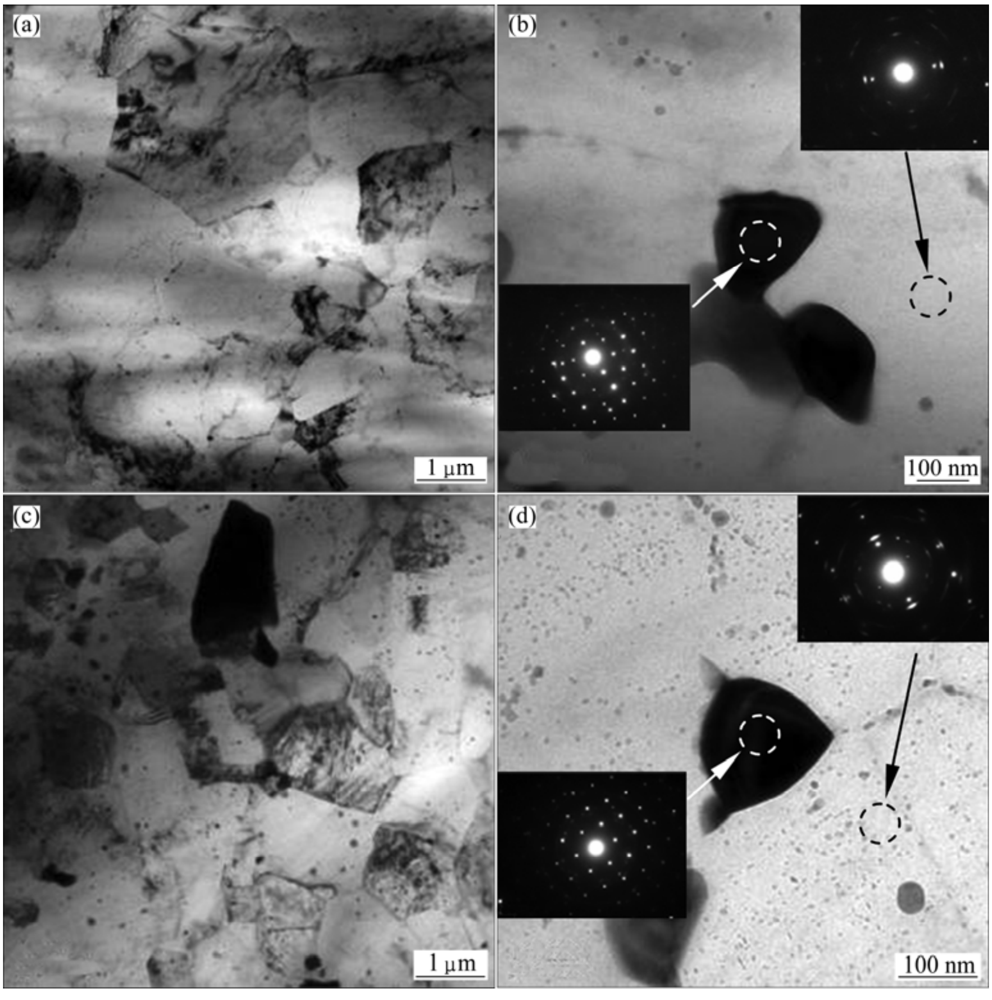

Fig. 9 TEM images of extruded ZK60−*x*Gd alloys: (a, b) ZK60; (c, d) ZK60−2.98Gd

the binding force between Zn and Gd is greater and then Gd atoms combine with Zn and Mg atoms to form Mg−Zn−Gd new phase on the priority. During the process, majority of Zn and Gd atoms in the melt are consumed, which leads to no formation of $MgZn_2$ and Mg−Gd binary phases for as-cast ZK60−2.98Gd alloy.

4.2 Grain refinement and dynamic recrystallization

Grain refinement mechanism for magnesium alloys has not been entirely clear, and is different for different grain-refining methods. However, the basic starting point is to increase the nucleation rate and inhibit the growth of crystal nuclei. Solute with good segregation and effective nuclei are two essential factors. Solute with good segregation can generate a solutal undercooling at the liquid−solid interface, impede the growth of dendrite and provide the driving force to activate the nucleation. Nucleation capacity of particles determines the start of solidification and number of effective nuclei at the solutal undercooling region. Role of solute element can be expressed by growth restriction factor (GRF) [2]. Metal Gd exhibits a relatively large value of growth restriction factor coefficient $m(k-1)$, i.e. 5.52, thus as-cast microstructure is refined effectively.

As a softening and grain-refining mechanism for magnesium alloys, dynamic recrystallization can ameliorate the deformation microstructure and enhance the mechanical property effectively. In the present work, large extrusion ratio (λ=40) can generate large deformation degree and ensure the adequate refinement of microstructures and occurrence of dynamic recrystallization. Middle extrusion temperature (T=593 K) can guarantee not only the occurrence of dynamic recrystallization, but also no easy growth of dynamic recrystallization grains. Low extrusion speed (v=1−2 m/min) can guarantee the fine microstructure. As-cast microstructure is refined gradually with increasing the Gd content, thus the corresponding dynamic recrystallization grains become smaller gradually. Increasing Mg−Zn−Gd phase can hinder the growth of dynamic recrystallization grains. Taking the above mentioned aspects into account, extruded microstructure is refined obviously and $\bar{d}$ decreases gradually to 2 μm for ZK60−2.98Gd alloy.

4.3 Strengthening mechanism

Grain-refinement strengthening is generally considered the most important strengthening mechanism for magnesium alloys [16,17]. In the present work, as-cast microstructure is refined gradually with increasing the Gd content. However, the second phase increases gradually and tends to distribute along grain boundary by continuous network. During the tensile deformation, dislocation piles at the interface between the second phase particles and α-Mg matrix, which can lead to stress concentration. When the stress reaches a certain degree, porosities and micro-cracks initiate. When it exceeds fracture strength, the matrix begins to fracture locally and plasticity decreases significantly. Taking the two aspects into account, as-cast tensile mechanical property is reduced slightly at ambient temperature when the Gd content does not exceed 2.98%.

Extruded microstructure is refined significantly and $\bar{d}$ decreases gradually to 2 μm for ZK60−2.98Gd alloy, which leads to the prominent strengthening effect by grain refinement. Meanwhile, fine dispersed Mg−Zn−Gd phase can also play a certain role in dispersion strengthening. Therefore, σ_b of extruded alloys can be enhanced significantly at ambient temperature and meanwhile increases gradually with increasing the Gd content. In addition, grain refinement is also favorable for ameliorating the ductility. However, the increasing second phase tends to distribute along the extrusion direction parallel to the tensile direction by zonal shape. Thus, δ decreases gradually and even is slightly lower than as-cast value for ZK60−2.98Gd alloy. In summary, it is necessary to avoid the distribution by continuous network in as-cast state or zonal shape in extruded state for the second phase.

For extruded ZK60 alloy, rare $MgZn_2$ phase plays a weak role in pinning grain boundary and leads to relatively poor tensile mechanical property at elevated temperatures, where σ_b decreases to 120 MPa at 473 K. With increasing the Gd content, Mg−Zn−Gd phase with a higher thermal stability increases gradually. Grain boundary is pinned and its sliding is inhibited effectively. Therefore, the tensile mechanical property is enhanced effectively at elevated temperatures, where σ_b increases to 164 MPa at 473 K for extruded ZK60−2.98Gd alloy.

5 Conclusions

1) With increasing the Gd content, Mg−Zn−Gd phase increases gradually, and $MgZn_2$ phase gradually decreases to disappear. The second phase tends to distribute along grain boundary by continuous network. As-cast microstructure is refined gradually, while its tensile mechanical property is reduced slightly at ambient temperature when the Gd content does not exceed 2.98%.

2) Extruded microstructure is refined obviously and $\bar{d}$ decreases gradually to 2 μm for ZK60−2.98Gd alloy. Broken second phase tends to distribute along the extrusion direction by zonal shape. Extruded tensile mechanical property is enhanced significantly at ambient and elevated temperatures. σ_b values at 298 and 473 K gradually increase from 355 and 120 MPa for ZK60

alloy to 380 and 164 MPa for ZK60−2.98Gd alloy, respectively. Extruded tensile fractures exhibit a typical character of ductile fracture.

3) The grain size and the second phase play an important role in affecting the tensile mechanical property of magnesium alloys.

References

[1] POLMEAR I J. Magnesium alloys and applications [J]. Materials Science and Technology, 1994, 10(1): 1−16.

[2] CHEN Zhen-hua. Wrought magnesium alloys [M]. Beijing: Chemical Industry Press, 2005: 1−20. (in Chinese)

[3] LUO Z P, SONG D Y, ZHANG S Q. Strengthening effects of rare earths on wrought Mg−Zn−Zr−RE alloys [J]. Journal of Alloys and Compounds, 1995, 230(2): 109−114.

[4] XU D K, LIU L, XU Y B, HAN E H. Effect of microstructure and texture on the mechanical properties of the as-extruded Mg−Zn−Y−Zr alloys [J]. Materials Science and Engineering A, 2007, 443(1−2): 248−256.

[5] LUO Su-qin, TANG Ai-tao, PAN Fu-sheng, SONG Kai, WANG Wei-qing. Effect of mole ratio of Y to Zn on phase constituent of Mg−Zn−Zr−Y alloys [J]. Transactions of Nonferrous Metals Society of China, 2011, 21(4): 795−800.

[6] XIA C Q, WANG Y N, WU A R, GU Y. Effects of cerium on microstructure and mechanical properties of ZK60 alloy [J]. Journal of Central South University of Technolnolgy, 2005, 12(5): 515−520.

[7] LI Q, WANG Q D, WANG Y X, ZENG X Q, DING W J. Effect of Nd and Y addition on microstructure and mechanical properties of as-cast Mg−Zn−Zr alloy [J]. Journal of Alloys and Compounds, 2007, 427(1−2): 115−123.

[8] YU W B, LIU Z Y, HE H, CHENG N P, LI X L. Microstructure and mechanical properties of ZK60−Yb magnesium alloys [J]. Materials Science and Engineering A, 2008, 478(1−2): 101−107.

[9] LI D Q, WANG Q D, DING W J. Effects of Ho on the microstructure and mechanical properties of Mg−Zn−Ho−Zr magnesium alloys [J]. Rare Metals, 2011, 30(2): 131−136.

[10] LI L, ZHANG X M, TANG C P, DENG Y L, ZHOU N. Mechanical properties and deep drawability of Mg−Gd−Y−Zr alloy rolling sheet at elevated temperatures [J]. Materials Science and Engineering A, 2010, 527(4−5): 1266−1274.

[11] ZHANG X M, LI L, DENG Y L, ZHOU N. Superplasticity and microstructure in Mg−Gd−Y−Zr alloy prepared by extrusion [J]. Journal of Alloys and Compounds, 2009, 481(1−2): 296−300.

[12] LIU X B, CHEN R S, HAN E H. Effects of ageing treatment on microstructures and properties of Mg−Gd−Y−Zr alloys with and without Zn additions [J]. Journal of Alloys and Compounds, 2008, 465(1−2): 232−238.

[13] WANG J, MENG J, ZHANG D P, TANG D X. Effect of Y for enhanced age hardening response and mechanical properties of Mg−Gd−Y−Zr alloys [J]. Materials Science and Engineering A, 2007, 456(1−2): 78−84.

[14] HUANG Zheng-hua, GUO Xue-feng, ZHANG Zhong-ming. Effects of Ce on damping capacity of AZ91D magnesium alloy [J]. Transactions of Nonferrous Metals Society of China, 2004, 14(2): 311−315.

[15] DEAN J A. Lange's handbook of chemistry [M]. 15th ed. New York: McGraw-Hill Press, 1999: 429−435.

[16] HALL E O. The deformation and ageing of mild steel: III. Discussion of results [J]. Proceedings of the Physical Society Section B, 1951, 64: 747−753.

[17] PETCH N J. The cleavage strength of polycrystals [J]. Journal of Iron Steel Institute, 1953, 174: 25−28.

Gd 对 ZK60 镁合金组织与力学性能的影响

黄正华，戚文军，徐 静

广州有色金属研究院，广州 510650

摘　要：分析了铸态和挤压态 ZK60−xGd(x=0~4)合金的组织和相组成，测试了其拉伸力学性能。结果表明，随着 Gd 含量的增加，铸态组织逐渐细化，Mg−Zn−Gd 新相逐渐增多，而 $MgZn_2$ 相逐渐减少直至消失，第二相趋于连续网状分布于晶界处；当 Gd 含量不超过 2.98%时，铸态室温拉伸力学性能稍降低。经挤压比λ=40 和挤压温度 T=593 K 的挤压后，组织显著细化，平均晶粒尺寸逐渐减至 ZK60−2.98Gd 合金的 2 μm，破碎的第二相沿着挤压方向呈带状分布；挤压态的拉伸力学性能均显著提高：298 和 473 K 时的抗拉强度分别从 ZK60 合金的 355 和 120 MPa 逐渐提高至 ZK60−2.98Gd 合金的 380 和 164 MPa。挤压态拉伸断口呈现典型的韧性断裂特征。

关键词：ZK60 镁合金；Gd 变质；挤压；显微组织；力学性能；断口形貌

(Edited by Hua YANG)